Supplementary Materials – OmniNet: Omnidirectional Jumping Neural Network with Height-awareness for Quadrupedal Robots

Abstract

This document has three sections. The first section mainly demonstrates the detailed computation process of computing the desired joint angle during aerial phase using the analytical Inverse Kinematic (IK) and the meaning of the involved variables [1]. The second section introduces the SHAP (SHapley Additive exPlanation) analysis that we conducted to illustrate the height estimator net's capability to accommodate the physical variation associated with height changing. In the third section, we include several experiments that show the omnidirectional jumping ability and robust landing ability of our jumping framework.

I. Analytical Inverse Kinematic

A foot height h_{feet} is predefined and set to be the same for each leg. Based on the theory in [1], we can compute the angle of calf, thigh, and hip respectively. Then we will calculate the velocity of each joint. In Table I, several geometrical properties of the robot are listed, which will be used to compute the calf angle.

TABLE I: Geometical Properties

Variables	Symbols	
hip origin	p^o_{hip}	$\mathbb{R}^3$
foot position	h_{feet}	$\mathbb{R}^3$
hip length	l_{hip}	$\mathbb{R}$
thigh length	l_{thigh}	$\mathbb{R}$
calf length	l_{calf}	$\mathbb{R}$

$$l_{ft} = \sqrt{l_{fh}^2 - l_{hip}^2} \tag{1}$$

$$l_{fh} = \sqrt{h_{feet}^2 - (p^o_{hip})^2} \tag{2}$$

$$\theta_{calf} = \arccos(\frac{l_{thigh}^2 + l_{calf}^2 - l_{ft}^2}{2 l_{thigh} l_{calf}} - \pi) \tag{3}$$

The relative angles of thigh and hip joint of the same leg are computed using some intermediate variables $\boldsymbol{u'}$,$\boldsymbol{v'}$, $\boldsymbol{u_t}$, $\boldsymbol{v_t}$, $\boldsymbol{u_h}$, $\boldsymbol{v_h}$, $\boldsymbol{\omega}$, $\boldsymbol{l_1}$, $\boldsymbol{l_2}$ and $\boldsymbol{r}$ which are gained through the robot's geometrical properties and predefined feet end-effector height h_{feet}, as follows:

TABLE II: Intermediate Variables

Variables	Symbols	
Relative position from foot to calf	p_{fc}	$\mathbb{R}^3$
Relative position from foot to thigh	p_{ft}	$\mathbb{R}^3$
A chosen point in the axis of hip joint	w_h	$\mathbb{R}^3$
Calf origin	p^o_{calf}	$\mathbb{R}^3$
Thigh origin	p^o_{thigh}	$\mathbb{R}^3$
Unit axis vector of thigh joint	w_t	$\mathbb{R}^3$
Unit axis vector of hip joint	w_h	$\mathbb{R}^3$
Relative position from foot to calf	p^o_{fc}	$\mathbb{R}^3$
Relative position from calf to thigh	p^o_{ct}	$\mathbb{R}^3$
Rotation matrix around the axis by its angle	$R_{axis}(\theta)$	$\mathbb{R}^{3\times3}$

$$p_{fc} = R_{\omega_{calf}}(\theta_{calf}) p^o_{fc} \tag{4}$$

$$v' = p^a_{hip} - p^o_{hip} \tag{5}$$

$$u' = p^o_{calf} + p_{fc} - p^o_{hip} \tag{6}$$

$$u_t = u' - \omega_t u'^T \omega_t \tag{7}$$

$$v_t = v' - \omega_t v'^T \omega_t \tag{8}$$

$$\delta = \sqrt{h_{feet}^2 - (p_{hip}^a)^2} \tag{9}$$

$$\delta' = \sqrt{\delta^2 - (\omega_t^T (p_{calf}^o + p_{fc} - p_{hip}^o - p_{hip}^a))^2} \tag{10}$$

$$\theta_1 = \arctan \frac{\omega_t^T u_t \times v_t}{u_t^T v_t} \tag{11}$$

$$\theta_2 = \arccos \frac{u_t^T u_t + v_t^T v_t - \delta'^2}{2||u_t||||v_t||} \tag{12}$$

$$\theta_{thigh} = \theta_1 - sign(\theta_1)\theta_2 \tag{13}$$

The deduction process of the hip angle is similar to that of thigh angle:

$$p_{fc} = R_{\omega_{thigh}}(\theta_{thigh}) p_{ct}^o + p_{fc} \tag{14}$$

$$v' = h_{feet} - p_{hip}^o \tag{15}$$

$$u' = p_{thigh}^o + p_{ft} - p_{hip}^o \tag{16}$$

$$u_h = u' - \omega_h u'^T \omega_h \tag{17}$$

$$v_h = v' - \omega_h v'^T \omega_h \tag{18}$$

$$\theta_{hip} = \arctan(\frac{\omega_h^T u_h \times v_h}{u_h^T v_h}) \tag{19}$$

For mapping between joint velocity and foot velocity, we have that the Jacobian velocity is always of full rank, as we exclude the singularity when computing the inverse kinematics.

$$p_{fh} = h_{feet} - p_{hip}^o \tag{20}$$

$$p_{ft} = \begin{bmatrix} -l_{\text{calf}} \sin(\theta_{calf}) \\ 0 \\ -l_{\text{calf}} \cos(\theta_{calf}) - l_{\text{thigh}} \end{bmatrix} \tag{21}$$

$$p_{fc} = \begin{bmatrix} 0 \\ 0 \\ -l_{\text{calf}} \end{bmatrix} \tag{22}$$

$$\tag{23}$$

$$J_{i,1} = -p_{fh} \times \begin{bmatrix} 1 \\ 0 \\ 0 \end{bmatrix} \tag{24}$$

$$J_{i,2} = -\mathbf{R}_x(\theta_{hip}) \cdot \mathbf{R}_y(\theta_{thigh}) \cdot \left(p_{ft} \times \begin{bmatrix} 0 \\ 1 \\ 0 \end{bmatrix} \right) \tag{25}$$

$$J_{i,3} = -\mathbf{R}_x(\theta_{hip}) \cdot \mathbf{R}_y(\theta_{thigh}) \cdot \mathbf{R}_y(\theta_{calf}) \cdot \left(p_{fc} \times \begin{bmatrix} 0 \\ 1 \\ 0 \end{bmatrix} \right) \tag{26}$$

$$\mathbf{J}_i = \begin{bmatrix} J_{i,1} & J_{i,2} & J_{i,3} \end{bmatrix} \tag{27}$$

Finally, Gaussian elimination is used to compute the joint velocity.

$$\begin{bmatrix} \dot{q}_{i,hip} \\ \dot{q}_{i,thigh} \\ \dot{q}_{i,calf} \end{bmatrix} = \mathbf{J}_i^{-1}(q_{i,hip}, q_{i,thigh}, q_{i,calf}) \begin{bmatrix} v_{i,x} \\ v_{i,y} \\ v_{i,x} \end{bmatrix}, i = 1, 2, 3, 4 \tag{28}$$

To ensure that the robot maintains its foot position and avoids leg extension, thereby preventing undesirable swinging foot behavior during the aerial phase, we set the target foot velocity relative to the body to zero at the peak of the motion, which inherently implies that the joint velocity must also be zero.

II. Attribute Analysis of the Height Estimator

The height estimator net's capability to accommodate the physical variation associated with height changing during the jumping process is examined. To explain the encoder function of the height estimator, the SHAP (SHapley Additive exPlanation) value [2] is implemented. The SHAP value of each component within the proprioception history $\boldsymbol{o}_i^j$ is calculated ($i \in \{1, ..., 20\}$ and $j \in \{1, ..., 46\}$). This value ϕ_i^j explains the contribution of $\boldsymbol{o}_i^j$ to the height estimator output $\boldsymbol{e}_t^\psi$. Fig. S1 visualizes the sum of the SHAP values of all observation components at each time instant i, i.e. $SHAP_i = \sum_j^{46} \phi_i^j$. The symbols used here are consistent with those in the manuscript.

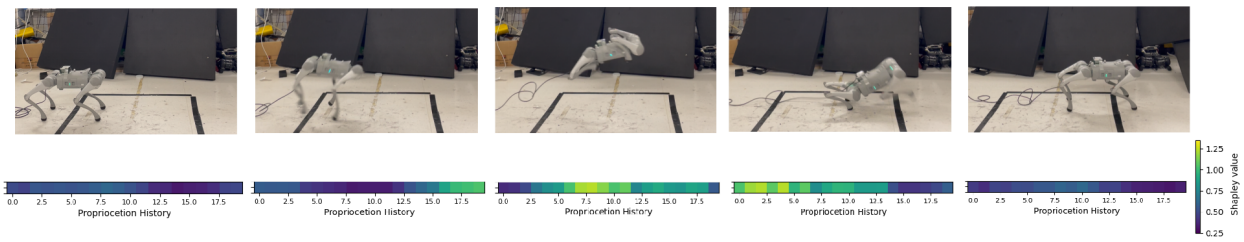

Fig. S1: A whole process of jumping, including prejump, flight, and landing phase. The SHAP value within a history buffer during the jumping process is described in the form of a heat map. The light yellow color grid represents a high SHAP value at that time. As the robot jumps, the SHAP values increase. After the robot lands, the SHAP values decrease to the normal standing phase level.

Through the heat map, it is clear to see that when the robot is in the normal state, each state in the proprioceptive history buffer contributes in a uniform manner to the prediction of the $\boldsymbol{e}_t^\psi$. When the robot enters the flight phase, the robot height h^{COM} change drastically. The observation $\boldsymbol{o}_t$ of this pivotal event exhibits the highest SHAP value when it is pushed back to the history buffer (20 slices of history states). During the jumping process, the robot's height and other proprioceptive properties largely change, which causes the input proprioception buffer of these time steps to contribute more significantly than the proprioception buffer at other time steps.

Moverover, higher SHAP values indicate that the jumping process significantly contributes to height estimation accuracy. Precise height estimation, in turn, enables the robot to determine the proper time to switch from the jumping states to the standing states.

III. Omnidirectinal Jumping Experiments

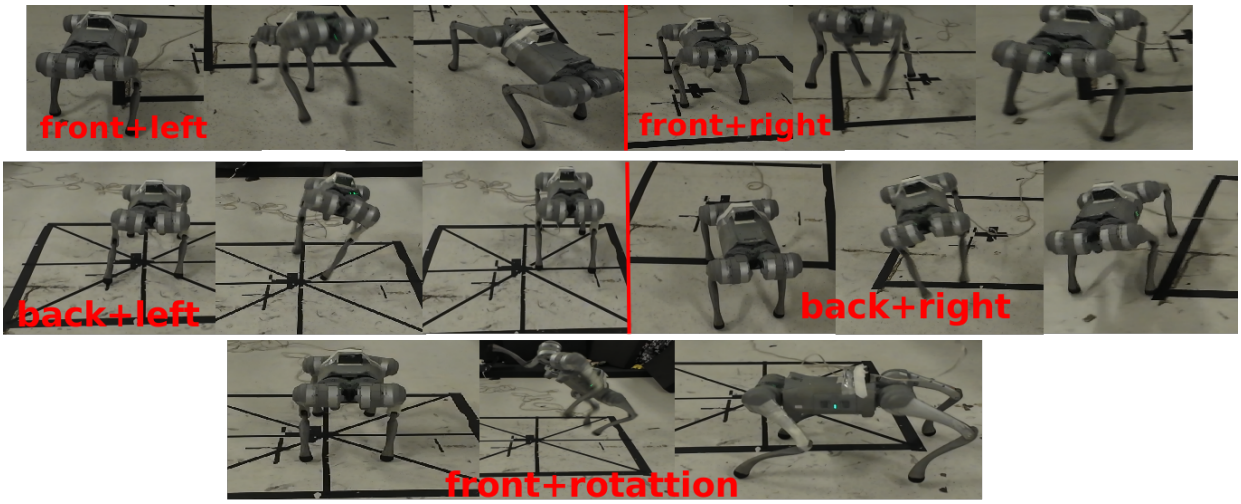

Fig. S2: Combound Directional Jumpings

As shown in Fig. S2, we have conducted some diagonal jump experiments that combine two directions together, including front right, front left, back right, back left, as well as the combinations of front and yaw-turning jump, which fully demonstrates our framework's omnidirectional jumping capabilities.

The Fig. S3 shows the results of robot landing on the soft and rough terrains, which has been mentioned in Section III-C of the manuscript. This experiment demonstrate the landing stability of out method.

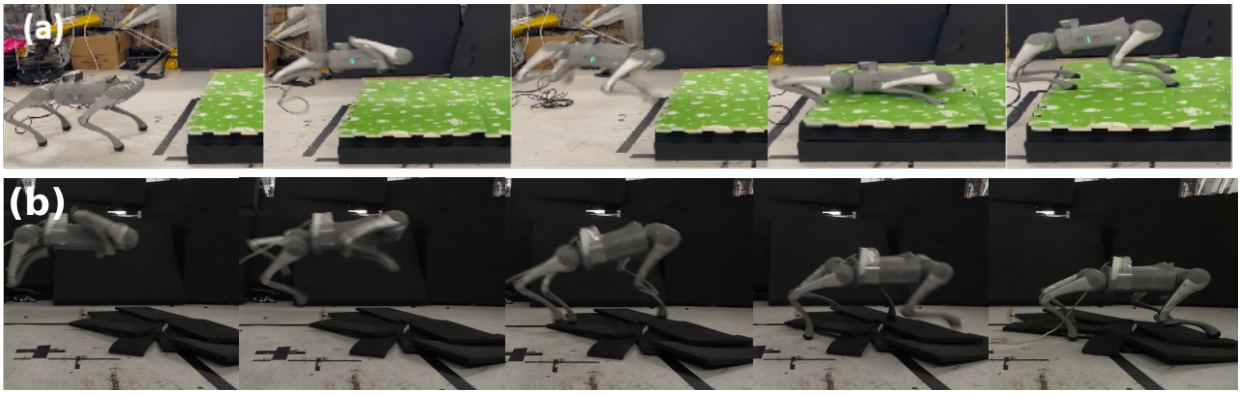

Fig. S3: (a) The robot lands on the soft terrain. (b) The robot lands softly on the rough terrain.

REFERENCES

[1] R. M. Murray, Z. Li, and S. S. Sastry, *A mathematical introduction to robotic manipulation*. CRC press, 2017.
[2] S. Lundberg and S.-i. Lee, "Shap: A unified approach to interpreting model predictions," *Advances in neural information processing systems*, pp. 1–10, 2017.